

IDENTIFICATION OF GENETIC FACTORS ASSOCIATED WITH CORPUS CALLOSUM MORPHOLOGY: CONDITIONAL STRONG INDEPENDENCE SCREENING FOR NON-EUCLIDEAN RESPONSES

BY ZHE GAO^{1,a}, JIN ZHU^{2,c}, YUE HU^{3,d}, WENLIANG PAN^{4,e} AND XUEQIN WANG^{1,b}

¹*School of Management, University of Science and Technology of China, ^agaozh8@mail.ustc.edu.cn; ^bwangxq20@ustc.edu.cn*

²*School of Mathematics, University of Birmingham, ^cj.zhu.7@bham.ac.uk*

³*Yale University School of Public Health ^dyue.hu@yale.edu*

⁴*State Key Laboratory of Mathematical Sciences, Academy of Mathematics and Systems Science, Chinese Academy of Sciences ^epanwliang@amss.ac.cn*

The corpus callosum, the largest white matter structure in the brain, plays a critical role in interhemispheric communication. Variations in its morphology are associated with various neurological and psychological conditions, making it a key focus in neurogenetics. Age is known to influence the structure and morphology of the corpus callosum significantly, complicating the identification of specific genetic factors that contribute to its shape and size. We propose a conditional strong independence screening method to address these challenges for ultrahigh-dimensional predictors and non-Euclidean responses, incorporating prior knowledge such as age through a novel concept of conditional metric dependence, which quantifies nonlinear conditional dependencies among random objects in metric spaces without relying on predefined models. We apply this framework to identify genetic factors associated with the morphology of the corpus callosum. Simulation results demonstrate the efficacy of this method across various non-Euclidean data types, highlighting its potential to drive genetic discovery in neuroscience.

1. Introduction. Neuroscience has seen transformative advancements, moving from basic anatomical studies to highly sophisticated computational analyses. The advent of neuroimaging technologies, such as magnetic resonance imaging (MRI), diffusion tensor imaging (DTI), and positron emission tomography (PET), has revolutionized the way we visualize and understand the brain's complex structures. These innovations have deepened our insights into neural anatomy and function while introducing non-Euclidean data that require novel analytical methods. One prominent example is the corpus callosum, the brain's largest white matter structure. Comprising approximately 200 million myelinated nerve fibers, it is the primary connection between the left and right hemispheres (Tanaka-Arakawa et al., 2015). These fibers form homotopic and heterotopic projections, enabling the integration and transfer of sensory, motor, and cognitive information between hemispheres (Kennedy, Van Essen and Christen, 2016). Changes in the size and shape of the corpus callosum can significantly impact its function and have been associated with several neurological conditions, including Alzheimer's disease (Bachman et al., 2014), schizophrenia, and bipolar disorder (Vermeulen et al., 2023).

The goal of genome-wide association studies (GWAS) that look into brain structure is to find out how genetic factors affect the structure and function of the brain. Researchers often collect high-dimensional genetic data and neurological metrics to do this. Along with genetic information, covariates like age and disease status are often included because they

Keywords and phrases: Conditional metric dependence, Conditional strong independence screening, Non-Euclidean response, Ultrahigh-dimensional data analysis.

significantly affect brain structure (Cornea et al., 2016; Biswal et al., 2010). However, the specific genetic factors that shape the morphology of the corpus callosum remain largely unexplored. Given the critical role of covariates like age in influencing corpus callosum structure, assessing the conditional contributions of genetic factors while adjusting for these covariates to identify key genetic determinants is essential. Identifying relevant factors from high-dimensional data while accounting for essential covariates remains crucial in analyzing non-Euclidean data.

To address the challenge of high-dimensional data analysis, Barut, Fan and Verhasselt (2016) introduced conditional sure independence screening (CSIS) within the generalized linear model framework, expanding upon the original sure independence screening (SIS) method (Fan and Lv, 2008). CSIS evaluates the conditional maximum likelihood estimator to measure marginal utility and selects variables with high marginal utility. Since its inception, CSIS has been adapted to various contexts. For instance, Hu and Lin (2017) developed an empirical-likelihood-based CSIS for less restrictive distributional assumptions, while Hong, Kang and Li (2018) introduced a version for censored responses. Furthermore, Chen et al. (2019) suggested a model-free version, and Wen et al. (2018) made a conditional distance correlation-based CSIS for responses with multiple variables. CSIS has also been extended to survival data (Lu, Chen and Wang, 2019). Other changes include an adaptive CSIS created by Lin and Sun (2016) to cut down on false positives and negatives, as well as robust CSIS methods for weaker model assumptions created by Hong, Wang and He (2016) and Zhang, Pan and Zhou (2018). Furthermore, Liu and Chen (2018) suggested a conditional quantile independence screening method to find features that affect the conditional quantiles of the response without defining a model structure, and Zheng, Hong and Li (2020) introduced a sequential conditioning method that updates the conditioning set over and over again.

Despite these numerous extensions, none of the existing CSIS methods are designed explicitly for non-Euclidean responses. This gap underscores the need for new approaches to handle the complex data structures encountered in modern neurogenetic studies.

This article aims to explore genetic factors influencing the shape of the corpus callosum by introducing a novel conditional screening method that addresses these gaps. Methodologically, we propose a model-free and distribution-free procedure called Conditional Metric Dependence-based Conditional Strong Independence Screening (COME-CSIS). Theoretically, COME-CSIS has been proven effective across a wide range of non-Euclidean data and exhibits strong screening properties in ultra-high-dimensional settings. In addition, COME-CSIS offers several significant advantages. It is robust, allowing for less restrictive moment conditions on both explanatory variables and the response. Its corresponding marginal utility enables conditional dependence analysis in non-Euclidean spaces, which has remained largely unexplored.

By applying COME-CSIS to both synthetic and real datasets, we demonstrate its ability to overcome the limitations of the strong negative type (Lyons, 2013), establishing it as a valuable tool for ultrahigh-dimensional non-Euclidean data analysis. In the real-data application, COME-CSIS was employed to identify genes associated with the shape of the corpus callosum. Compared to existing screening methods, our approach avoided selecting genes related primarily to age or Alzheimer’s disease, which are well-known factors influencing corpus callosum morphology. These results provide important preliminary insights into the gene regulation mechanisms affecting the corpus callosum and open the door for further investigation.

The following contents are organized as follows: In Section 2, we introduce notation and formulate our problem. Then, we propose a novel marginal utility for CSIS and a related CSIS procedure and study their theoretical properties in Section 3. In Section 4, we conduct simulation studies to evaluate the performance of our method. In Section 5, we analyze a real-world dataset to demonstrate the helpfulness of our method. Finally, we conclude this article

with a few remarks in Section 6. All of the technical details are deferred to the supplementary materials.

2. Preliminaries. The section will introduce notations and formulate our problem in subsection 2.1 and 2.2, respectively.

2.1. *Notations.* Let (X, Y, Z) be a random variable defined on a probability space, where $Y \in \mathcal{Y}$ is a metric-valued variable, and X, Z are Euclidean-valued variables with respective dimensionalities d and d_z . We decompose X into p variables, denoted as $X = (X_1, \dots, X_p)$, where each component X_i has dimensionality d_i , satisfying $\sum_{i=1}^p d_i = d$. Assume that the regular conditional probabilities of $(X_1, Y), \dots, (X_p, Y)$, and (X_1, \dots, X_p, Y) given Z exist.

To facilitate the analysis of the variable Y in the non-Euclidean space \mathcal{Y} , we introduce the following notation and assumptions. Suppose (\mathcal{Y}, ρ) is a Polish space, endowed with a metric ρ . Let $\bar{B}_{\mathcal{Y}}(u, v)$ represents a closed ball centered at u with radius $r = \rho(u, v)$. An analogous definition applies to the closed balls in the Euclidean space \mathbb{R}^d where X is located. The product metric space is defined as $(\mathbb{R}^d \times \mathcal{Y}, \rho_{\mathbb{R}^d \times \mathcal{Y}})$. Denote the regular conditional probabilities of $(X, Y), X, Y$ given Z as $\mu_{XY|Z}, \mu_{X|Z}, \mu_{Y|Z}$.

We further restrict the space (\mathcal{Y}, ρ) by introducing the following definition:

DEFINITION 1 (Federer (2014)). A metric ρ is called directionally (ϵ, η, L) -limited at the subset A of \mathcal{Y} , if $\epsilon > 0, 0 < \eta \leq 1/3, L$ is a positive integer, and the following condition holds: if for each $a \in A, D \subseteq A \cap \bar{B}_{\mathcal{Y}}(a, \epsilon)$ such that $\rho(x, c) \geq \eta\rho(a, c)$ whenever $b, c \in D, b \neq c, x \in \mathcal{Y}$ with

$$\rho(a, x) = \rho(a, c), \rho(x, b) = \rho(a, b) - \rho(a, x)$$

then the cardinality of D is no larger than L .

Directionally (ϵ, η, L) -limited stipulates that the directionality at each local point must be finite. More details can be found in (Federer, 2014; Wang et al., 2024).

Let $\{(X_{1i}, \dots, X_{pi}, Y_i, Z_i)\}_{i=1}^n$ be an *i.i.d.* sample of (X_1, \dots, X_p, Y, Z) . Suppose $I(\cdot)$ is an indicator function, we define $\delta_{ij,k}^{X_r} = I(X_{rk} \in \bar{B}_{\mathbb{R}^{d_r}}(X_{ri}, X_{rj}))$, which indicates whether X_{rk} is located in $\bar{B}_{\mathbb{R}^{d_r}}(X_{ri}, X_{rj})$, and $\delta_{ij,kl}^{X_r} = \delta_{ij,k}^{X_r} \delta_{ij,l}^{X_r}$, which is an indicator for whether both of X_{rk} and X_{rl} fall into $\bar{B}_{\mathbb{R}^{d_r}}(X_{ri}, X_{rj})$. Also, let $\eta_{ij,klst}^{X_r} = (\delta_{ij,kl}^{X_r} + \delta_{ij,st}^{X_r} - \delta_{ij,ks}^{X_r} - \delta_{ij,lt}^{X_r})/2$. Analogously, define the notations $\delta_{ij,k}^Y, \delta_{ij,kl}^Y$ and $\eta_{ij,klst}^Y$ for Y . The product of $\eta_{ij,klst}^{X_r}$ and $\eta_{ij,klst}^Y$ is defined as $\zeta_{ijklst,r} = \eta_{ijklst}^{X_r} \eta_{ijklst}^Y$.

2.2. *Problem formulation.* The primary objective of this article is to establish a conditional sure independence screening method for identifying relevant factors from high-dimensional data, particularly when considering response variables in the analysis of non-Euclidean data. Consider the random objects (X_1, \dots, X_p, Y, Z) defined previously, where p is large, indicating that only a small fraction of the X variables are relevant to Y given Z . We characterize this relevance through conditional independence: if $X_r \perp Y \mid Z$, then the variable X_r is deemed unnecessary. Conversely, if $X_r \not\perp Y \mid Z$, then X_r is considered necessary. Here, \perp and $\not\perp$ denote conditional independence and dependence, respectively.

We define the inactive set and active set as follows:

$$\mathcal{I} = \{r \mid r \in \{1, \dots, p\} \text{ and } X_r \perp Y \mid Z\},$$

$$\mathcal{A} = \{r \mid r \in \{1, \dots, p\} \text{ and } X_r \not\perp Y \mid Z\}.$$

Our goal is to accurately identify the set \mathcal{A} . Returning to the real-world problem discussed in the previous section, consider Y as the shape of the corpus callosum, and each X_i (for $i = 1, \dots, p$) as a genetic factor. Z includes confounding variables that are presumed to influence the relationship between the shape of the corpus callosum and genetic factors, such as age, gender, and disease status. Our objective is to detect the genetic factors that are truly associated with the shape of the corpus callosum while accounting for these confounding variables, effectively recovering the set \mathcal{A} .

3. Methods. In this section, we systematically introduce the measure of conditional independence for general spaces and the screening process developed based on this measure. Additionally, we delineate the theoretical properties that substantiate the efficacy of the proposed method.

3.1. *Conditional metric dependence (COME).* We will present two types of conditional metric dependence (COME): conditional ball covariance and global conditional ball correlation in this part. Our key idea for the COME measures is to evaluate the difference between $\mu_{XY|Z}$ and the product measure of $\mu_{X|Z}$ and $\mu_{Y|Z}$ on the close ball set. We first present the definitions of conditional ball covariance.

DEFINITION 2. The conditional ball covariance is defined as

$$\mathcal{V}^2(X, Y|Z) = \int [\mu_{XY|Z}(\bar{B}_{\mathbb{R}^d}(x_1, x_2) \times \bar{B}_{\mathcal{Y}}(y_1, y_2)) - \mu_{X|Z}(\bar{B}_{\mathbb{R}^d}(x_1, x_2))\mu_{Y|Z}(\bar{B}_{\mathcal{Y}}(y_1, y_2))]^2 \times \mu_{XY|Z}(dx_1, dy_1)\mu_{XY|Z}(dx_2, dy_2).$$

Notably, $\mathcal{V}^2(X, Y|Z)$ is a non-negative random variables of Z . It evaluates the conditional dependence between X and Y for all points in the support set of Z , and thus, it can be considered as a “local” conditional dependence measure. Similar to the traditional correlation coefficient, we can also define the conditional ball correlation

DEFINITION 3. The conditional ball correlation is defined as

$$\mathcal{R}^2(X, Y|Z) = \frac{\mathcal{V}^2(X, Y|Z)}{\sqrt{\mathcal{V}^2(X, X|Z)\mathcal{V}^2(Y, Y|Z)}}.$$

if $\mathcal{V}^2(X, X|Z)\mathcal{V}^2(Y, Y|Z) > 0$, and 0 otherwise.

Next, we present a “global” measure for conditional dependence by take expectation on the condition variable Z .

DEFINITION 4. The global conditional ball correlation is

$$\tau = E[\mathcal{R}^2(X, Y|Z)].$$

The metrics defined in Definitions 2 and 4 are pivotal to our analysis and are utilized to quantify the correlation between random variables X and Y , conditioned on Z . The conditional ball covariance specifically measures local conditional correlations given Z . However, $\mathcal{R}^2(X, Y|Z)$ is a function of Z , it is not directly suitable for ranking purposes and may not be suitable as a marginal utility function in certain scenarios. Back to the previous application problem, when examining the relationship between the shape of the corpus callosum and specific genes, conditioned on age, the global conditional ball correlation is the appropriate

metric. Conversely, when the focus is strictly on the population aged 60, conditional ball covariance should be applied directly.

We turn to show that the two COME measures are proper conditional dependence measures under mild conditions. Our first condition is related to probability measures. Let \mathbf{M}_1 be a collection of discrete Borel probability measures on $\mathbb{R}^d \times \mathcal{Y}$, and \mathbf{M}_2 be a collection of Borel probability measures on $\mathbb{R}^d \times \mathcal{Y}$ such that $\forall (x_1, y_1) \in \mathbb{R}^d \times \mathcal{Y}$ and $(x_2, y_2) \sim \mu_{XY|Z}, (\rho_{\mathbb{R}^d}(x_1, x_2), \rho_{\mathcal{Y}}(y_1, y_2))$ has a continuous density function. The first condition is:

(C1) Both $\mu_{X|Z}$ and $\mu_{Y|Z}$ are convex combinations of elements in \mathbf{M}_1 and \mathbf{M}_2 .

Our second condition relies on the restriction of (\mathcal{Y}, ρ) :

(C2) ρ is directionally- (ϵ, η, L) limited at \mathcal{Y} .

The essence of the conditional independence measure is based on comparing differences across a set of closed balls. This approach allows our method to be effectively applied in complex spaces, exhibiting desirable performance. The foundational attribute of these desirable properties lies in the finite covering theorem for closed balls. This theorem is akin to the Vitali covering theorem in Euclidean spaces, which is crucial for establishing the correspondence theorem. Condition (C2) is essential to ensure that the covering theorem remains valid in the complex space \mathcal{Y} . Specifically, (C2) mandates that directionality at each local point is finite. We further illustrate the applicability of the modified (C2) with examples such as finite-dimensional Banach spaces equipped with a norm, finite-dimensional Riemannian manifolds with bounded sectional curvature, and metric spaces corresponding to binary phylogenetic trees with a fixed number of leaves. Given that X resides in a Euclidean space, condition (C2) is naturally satisfied. Condition (C1) ensures that, within the framework of a product space, the directionality constraints of each space are sufficient to uphold the covering theorem. Concurrently, sets \mathbf{M}_1 and \mathbf{M}_2 cover the majority of the measure, which is not an overly stringent assumption. As far as we know, these two conditions cannot be relaxed, otherwise counterexamples can be given. For a more detailed discussion, please refer to (Wang et al., 2024).

The theorem below guarantees the COME measures are proper measurements for conditional dependence.

THEOREM 1. *If (C1) and (C2) hold, the following properties hold:*

- (i) $\mathcal{V}^2(X, Y|Z) \geq 0$ almost surely, and the equality holds if and only if $X \perp\!\!\!\perp Y|Z$.
- (ii) $0 \leq \tau \leq 1$, and $\tau = 0$ if and only if $X \perp\!\!\!\perp Y|Z$.

Theorem 1 shows that, under mild conditions, $\mathcal{V}^2(X, Y|Z) \stackrel{a.s.}{=} 0$ and $\tau = 0$ are equivalent to conditional independence. Many well-known conditional independence measures satisfy similar conditional-independence equivalence, like the kernel conditional dependence measures (Fukumizu et al., 2008) and the conditional distance correlation (Wang et al., 2015). Many metric spaces encountered in non-Euclidean data analysis are directionally limited, such as Riemannian manifolds and phylogenetic tree spaces (Wang et al., 2024).

Theorem 1 offers a theoretical guarantee for our analytical procedures. Specifically, when employing the COME technology, this theorem ensures that irrelevant variables are not detected. In the absence of Theorem 1, the application of COME to analyze the shape of the corpus callosum could inadvertently lead to the selection of genes that have no relevance to the corpus callosum (CC) shape. Such an occurrence would undermine the credibility of our results and pose challenges for subsequent research endeavors.

For practical usage, we propose the COME estimators. We first show that the conditional ball covariance is the conditional expectation of two random variables:

THEOREM 2. *A variable-separated variant of the conditional ball covariance is given as follows,*

$$\mathcal{W}^{X,Y}(z) = E\{\eta_{12,3456}^X \eta_{12,3456}^Y | Z_1, \dots, Z_6 = z\}.$$

Theorem 2 motivates us to estimate τ with V-processes and density estimation of Z . Denote H and $K(\cdot)$ as bandwidth matrix and kernel function, respectively. Let $\hat{f}_k(z) = (n|H|)^{-1}K(H^{-1}(z - Z_k))$, the kernel density estimation for $Z = z$ is presented as $\hat{f}(z) = \sum_{k=1}^n \hat{f}_k(z)$. Then $\mathcal{W}^{X,Y}(z)$ can be estimated by the empirical V-process:

$$\mathcal{W}_n^{XY}(z) = \sum_{i,j,k,l,s,t=1}^n \frac{\hat{f}_i(z)\hat{f}_j(z)\hat{f}_k(z)\hat{f}_l(z)\hat{f}_s(z)\hat{f}_t(z)}{\hat{f}^6(z)} \eta_{ijklst}^X \eta_{ijklst}^Y.$$

And $\mathcal{R}^2(X, Y | Z = z)$ can be estimated by:

$$\mathcal{R}_n^2(X, Y | Z = z) = \mathcal{W}_n^{XY}(z) / \sqrt{\mathcal{W}_n^{XX}(z)\mathcal{W}_n^{YY}(z)},$$

if $\mathcal{W}_n^{XX}(z)\mathcal{W}_n^{YY}(z) > 0$, and 0 otherwise. From the definition of τ , it can be estimated by

$$(1) \quad \hat{\tau} = \frac{1}{n} \sum_{u=1}^n \mathcal{R}_n^2(X, Y | Z = z_u).$$

The computation burden would be extremely heavy if computing $\hat{\tau}$ according to its exact definition (1). In supplementary material, we will develop a method to significantly reduce the time complexity of computing $\hat{\tau}$.

3.2. COME based conditional strong independence screening. The subsection establishes a novel CSIS procedure to tackle the problem formulated in subsection 2.2. According to Theorem 1, under mild conditions, the global ball condition correlation equal to zero is equivalent to the conditional independence thereby, we have:

$$\mathcal{A} = \{r \mid \tau_r > 0\} \text{ and } \mathcal{I} = \{r \mid \tau_r = 0\},$$

where τ_r is the global conditional ball correlation between X_r and Y given Z . This fact motivates us to calculate the global conditional ball correlation for pair (X_r, Y, Z) as a marginal utility to assess the influence of X_r on the response Y given Z , and then filter out the variables with zero global conditional metric dependence. Based on this motivation, we propose a two-step procedure, COME-based conditional strong independence screening (COME-CSIS):

- (i) Given a dataset $\{(X_{1i}, \dots, X_{pi}, Y_i, Z_i)\}_{i=1}^n$, we compute $\hat{\tau}_1, \dots, \hat{\tau}_p$ according to (1);
- (ii) Using $\hat{\tau}_i$ as a marginal utility, we select the X_r that fall into

$$\hat{\mathcal{M}}_{d_n} = \{r \mid \hat{\tau}_r > \tau_n, r = 1, \dots, p\}.$$

where τ_n is a pre-specified constant.

In practical applications, we also recommend using the hard threshold method to truncate $\hat{\tau}_1, \dots, \hat{\tau}_p$, that is, select the first d_n variables, where d_n is related to n (Fan and Lv, 2008).

$$\hat{\mathcal{M}}_{d_n} = \{r \mid \hat{\tau}_r \text{ is the first } d_n \text{ largest of } \{\hat{\tau}_1, \dots, \hat{\tau}_p\}\}.$$

Next, we study the strong screening property of the COME-CSIS, which ensures that $\hat{\mathcal{M}}_{d_n} = \mathcal{A}$ with high probability. The strong screening property asserts a more desirable result than the sure screening property, which only guarantees $\mathcal{A} \subseteq \hat{\mathcal{M}}_{d_n}$. Such a property is also for recently advanced screening methods such as Huang, Li and Wang (2014) and Pan

et al. (2019). As a demonstration, we apply the COME-CSIS method to synthetic datasets as described in Section 4.1, setting $d_n = 3$. We compare this approach with BCor-SIS (Pan et al., 2019) and CDC-SIS (Wen et al., 2018). The proportion of $\hat{\mathcal{M}}_{d_n} = \mathcal{A}$ is depicted in Figure 1. According to Figure 1, the likelihood that our proposed method precisely identifies set \mathcal{A} approaches unity as the sample size increases. Concurrently, the performance of our method surpasses that of the methods compared.

To derive the strong screening of the COME-CSIS, we impose some conditions as follows.

(C3) The kernel function $K(\cdot)$ is non-negative and uniformly-bounded, and the bandwidth for kernel estimation of Z satisfies $h = O(n^{-\kappa/(2d_z)})$, where $0 \leq \kappa < 1/2$.

(C4) If Z_1, \dots, Z_6 are independent copies of Z , then for $1 \leq r \leq p$, there exists a positive constant L , such that

$$\max_r |E(\zeta_{123456,r} | Z_1, Z_2, Z_3, Z_4, Z_5, Z_6) - E(\zeta_{123456,r} | Z'_1, Z_2, Z_3, Z_4, Z_5, Z_6)| \leq L \|Z_1 - Z'_1\|.$$

(C5) There exists a positive constant s_0 such that for all $0 < s \leq s_0$ and $z \in \text{supp}\{Z\}$,

$$E[\exp(sK_H(Z - z)\|Z - z\|)] < \infty.$$

(C6) There exist some constants $c > 0$ and $0 \leq \kappa < 1/2$ such that

$$\min_{r \in \mathcal{A}} \tau_r \geq 2cn^{-\kappa}.$$

Condition (C3) imposes a mild condition on the kernel function, and most existing kernel functions satisfy this regularity condition. It also claims that the bandwidth of kernel estimation of Z satisfies $h = O(n^{-\kappa/(2d_z)})$. This requirement for bandwidth helps guarantee the density estimate is consistent. The works of Liu, Li and Wu (2014) and Wen et al. (2018) also rely on similar conditions. To make condition (C3) hold, the kernel function is set as a rectangle kernel, and its bandwidth is set as $h = n^{-1/(6d_z)}$ in our implementation. Condition (C4) is satisfied if the first order partial derivative of $E(\zeta_{123456,r} | Z_1, Z_2, Z_3, Z_4, Z_5, Z_6)$ are all bounded, which is similar to one of condition in Wen et al. (2018). Condition (C5) provides an exponential bound on the product of kernel function and the distance of variable Z . Condition (C6) assumes that the minimum true signal has a lower bound with the order of $n^{-\kappa}$, which still allows the minimum true signal to approach zero when the sample size n increases infinity. Assumptions analogous to condition (C6) are common in the high-dimensional data analysis literature (e.g., Meinshausen and Bühlmann (2006), Fan and Lv (2008), Barut, Fan and Verhasselt (2016), Xue and Liang (2017)). Under these conditions, the following theorem presents the strong screening property of the COME-CSIS:

THEOREM 3 (Strong screening property of the COME-CSIS). *If both the conditions in Theorem 1 and conditions (C3)-(C5) hold, then for any $\tau_n \in (0, 2cn^\kappa)$, $0 < \gamma < 1/2 - \kappa$, there exists positive constants c_1 and c_2 such that*

$$\mathbb{P}(\max_{1 \leq r \leq p} |\hat{\tau}_r - \tau_r| \geq cn^{-\kappa}) \leq p[\exp(-c_1 n^{1-2(\gamma+\kappa)}) + n^6 \exp(-c_2 n^\gamma)] + o(1).$$

If condition (C6) also holds, we have

$$\mathbb{P}(\mathcal{A} \subseteq \hat{\mathcal{M}}_{d_n}) \geq 1 - |\mathcal{A}|[\exp(-c_1 n^{1-2(\gamma+\kappa)}) + n^6 \exp(-c_2 n^\gamma) + \exp(-c_3 n^{1-2\kappa})] + o(1),$$

$$\mathbb{P}(\hat{\mathcal{M}}_{d_n} \subseteq \mathcal{A}) \geq 1 - d_n[\exp(-c_1 n^{1-2(\gamma+\kappa)}) + n^6 \exp(-c_2 n^\gamma) + \exp(-c_3 n^{1-2\kappa})] + o(1),$$

where $|\mathcal{A}|$ is the size of the set \mathcal{A} and c_3 is a positive constant. If $\log p = o(n^{\min\{1-2(\gamma+\kappa), \gamma\}})$, then the strong screening consistency holds,

$$\mathbb{P}(\hat{\mathcal{M}}_{d_n} = \mathcal{A}) \xrightarrow{a.s.} 1 \text{ when } n \rightarrow \infty.$$

Theorem 3 claims that, without specifying a model among X_r, Y , and Z , the COME-CSIS enjoys the strong screening property for the directionally limited metric space-valued response. Thus, it works for data in typical non-Euclidean spaces like separable Banach spaces, Riemannian manifolds, etc. The COME-CSIS imposes no moment assumption on X_1, \dots, X_p and Y , and thus, it is robust to heavy-tailed observations and the presence of potential outliers appearing in these variables. This property is beneficial for high-dimensional data analysis because it is rigorous to assume all explanatory variables are well-behavior when p is large. Theorem 3 also provides a theoretical guarantee for accurately selecting all relevant factors when analyzing non-Euclidean response variables in real applications.

As a complementary, we discuss determining the model size d_n . Generally speaking, it involves conducting a conditional independence test, a tough hypothesis test (Shah and Peters, 2020). Fortunately, if we assume the dependence between Y and (X, Z) follows one of the models: global Fréchet regression (Petersen and Müller, 2019), geodesic regression (Fletcher, 2013) or intrinsic regression (Cornea et al., 2016), then we could stop adding a new predictor when it does not statistically affect the interpretation of the variation of Y . This effect can be measured by a generalization of the adjusted coefficient of determination for the global Fréchet regression and geodesic regression, or a Wald-type test statistic for the intrinsic regression model.

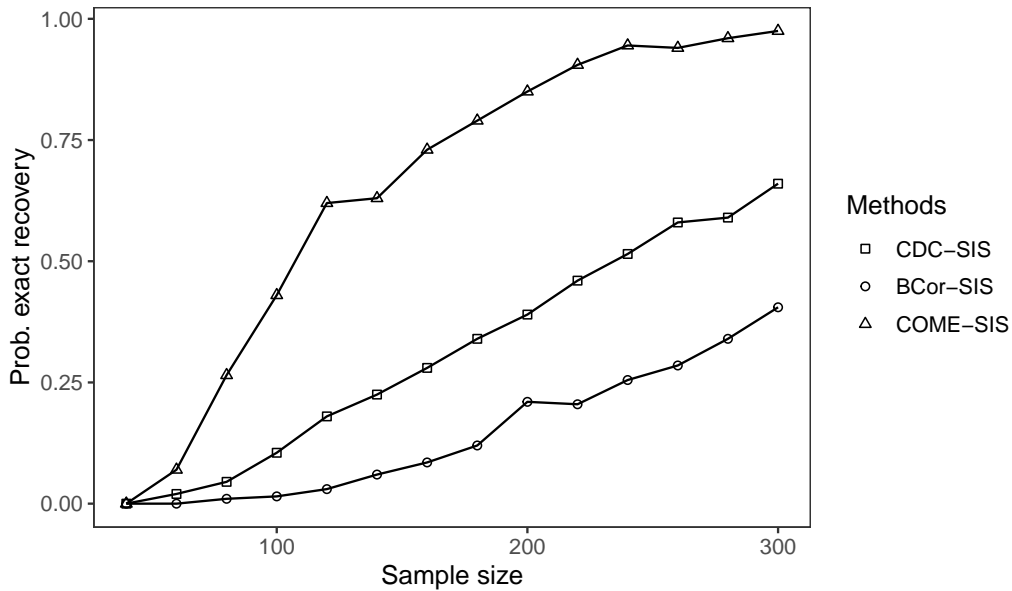


Fig 1: Plot of the probability $\mathbb{P}(\hat{\mathcal{M}}_{d_n} = \mathcal{A})$ versus the sample size under Model (1.b) with $d_n = 3$, described in Section 4.1.

4. Simulation. In this section, we investigate the empirical performance of the COME-CSIS by synthesis datasets. We evaluate the COME-CSIS by the proportion P_i that it correctly includes the effective variable X_i under a given model size d_n in the R replications (Li, Zhong and Zhu, 2012). We also consider the proportion P_a that all effective variables are selected simultaneously. If the screening procedure works well, P_i s and P_a should be close to 1. We fix the sample size n at 150, the dimension p at 2000, and the number of replications R at 100. We set the model size $d = \gamma \lceil n / \log(n) \rceil$ as Li, Zhong and Zhu (2012) suggested,

where $\lceil a \rceil$ refers to the integer part of a and γ 's value is 1, 2, or 3. For comparison, the BCor-SIS (Pan et al., 2019) and CDC-SIS (Wen et al., 2018) are taken into consideration, and two R packages: Ball and cdcsis (Zhu et al., 2021; Hu et al., 2019) are used to perform the two screening procedures. Since the CDC-SIS also relies on kernel density estimation, for fairness, the kernel function and its bandwidth used in the CDC-SIS is controlled to be the same as that of the COME-CSIS.

We consider two common data types of non-Euclidean response: functional data and directional data, in Section 4.1 and Section 4.2, respectively. As a complementary, the study of the classical Euclidean response is deferred to the supplementary material. For the conditional variable and explanatory variables (Z, X_1, \dots, X_p) , they are jointly sampled from a multivariate normal distribution with zero means and covariance matrix Σ where $\Sigma_{ij} = 2\rho^{|i-j|}$. The value of ρ may be 0.0 or 0.7.

4.1. *Functional curve data.* First, we entail the procedure for synthesizing the functional curve response. Suppose $B_1(t), \dots, B_4(t)$ are four B-spline basis functions, we generate the a response Y as the linear combination of the basis functions, where the linear coefficients are related to Z, X_1, X_3, X_6 . We consider the following two models. The first model is a generalized additive model, and the second one is an interaction model:

$$(1.a): Y(t) = ZB_1(t) + X_1B_2(t) + X_3B_3(t) + X_6^2B_4(t) + \epsilon(t);$$

$$(1.b): Y(t) = ZB_1(t) + 2X_1X_3B_2(t) + ZX_3B_3(t) + ZX_6B_4(t) + \epsilon(t).$$

$\epsilon(t)$ is a zero-mean Gaussian process in these two models. The functional curve $Y(t)$ is observed in 17 equally spaced points at interval $[0, 8\pi]$. To conduct the three screening procedures, L_2 norm (Febrero-Bande and de la Fuente, 2012) are used to measure the dissimilarity of two functional observations.

The results on functional data are displayed in Table 1. For Model (1.a), the three methods have a high probability of identifying the true variables, and both CDC-SIS and BCor-SIS are slightly better than the COME-CSIS. The CDC-SIS surpasses COME-CSIS because distance correlation-based methods have strong power in detecting the linear relationship (Pan et al., 2020); BCor-SIS has better power because the effect of the conditional variable Z can be considered additive noise. In Model (1.b), the COME-CSIS turns into the most powerful method and has a much larger chance to detect all influential variables simultaneously when $\rho = 0$. It is also worth noting that BCor-SIS has limited power to detect the influential variable X_6 that interacts with the conditional variable.

4.2. *Directional data.* We consider two models for generating directional data. The first model generates observations in a unit sphere, while the second generates observations in a unit circle. In the following, $U_c(a, b)$ represents a uniform distribution on the unit circle, where a and b are the lower and upper bound of the radian. The two models are:

$$(2.a): \phi = ZX_3, \theta = \frac{1}{2}(X_6 + X_9)$$

$$Y = (\sin \theta \cos \phi, \cos \theta \sin \phi, \cos \theta).$$

$$(2.b): \omega_1, \omega_2, \omega_3 \text{ are } i.i.d \text{ Bernoulli random variables with } \frac{1}{2} \text{ probability to take value 1,}$$

TABLE 1
The selection proportion of effective variables in functional data

ρ	γ	Methods	Model (1.a)				Model (1.b)			
			P_1	P_3	P_6	P_a	P_1	P_3	P_6	P_a
0.0	d_1	CDC-SIS	1.00	1.00	1.00	1.00	0.75	0.99	1.00	0.75
	d_2	BCor-SIS	1.00	0.99	1.00	0.99	0.93	1.00	0.48	0.43
	d_3	COME-CSIS	0.97	0.93	1.00	0.90	0.97	1.00	1.00	0.97
	d_1	CDC-SIS	1.00	1.00	1.00	1.00	0.83	1.00	1.00	0.83
	d_2	BCor-SIS	1.00	1.00	1.00	1.00	0.96	1.00	0.61	0.58
	d_3	COME-CSIS	0.99	0.97	1.00	0.96	0.98	1.00	1.00	0.98
	d_1	CDC-SIS	1.00	1.00	1.00	1.00	0.88	1.00	1.00	0.88
	d_2	BCor-SIS	1.00	1.00	1.00	1.00	0.98	1.00	0.71	0.69
	d_3	COME-CSIS	0.99	0.98	1.00	0.97	0.98	1.00	1.00	0.98
0.7	d_1	CDC-SIS	1.00	1.00	1.00	1.00	1.00	1.00	1.00	1.00
	d_2	BCor-SIS	1.00	1.00	1.00	1.00	1.00	1.00	0.51	0.51
	d_3	COME-CSIS	0.96	1.00	1.00	0.96	0.99	1.00	1.00	0.99
	d_1	CDC-SIS	1.00	1.00	1.00	1.00	1.00	1.00	1.00	1.00
	d_2	BCor-SIS	1.00	1.00	1.00	1.00	1.00	1.00	0.60	0.60
	d_3	COME-CSIS	0.97	1.00	1.00	0.97	1.00	1.00	1.00	1.00
	d_1	CDC-SIS	1.00	1.00	1.00	1.00	1.00	1.00	1.00	1.00
	d_2	BCor-SIS	1.00	1.00	1.00	1.00	1.00	1.00	0.71	0.71
	d_3	COME-CSIS	0.99	1.00	1.00	0.99	1.00	1.00	1.00	1.00

$$Y = \begin{cases} \omega_1 U_c(0, \frac{\pi}{6}) + (1 - \omega_1) U_c(\pi, \frac{7\pi}{6}), & \text{if } Z' = 1, X'_3 = I(X_3 > \text{median}(X_3)) \\ \omega_1 U_c(\frac{\pi}{2}, \frac{2\pi}{3}) + (1 - \omega_1) U_c(\frac{3\pi}{2}, \frac{5\pi}{3}), & \text{if } Z' = 1, X'_3 = I(X_3 \leq \text{median}(X_3)) \\ \omega_2 U_c(\frac{\pi}{6}, \frac{\pi}{3}) + (1 - \omega_2) U_c(\frac{7\pi}{6}, \frac{4\pi}{3}), & \text{if } Z' = 2, X'_6 = I(X_6 > \text{median}(X_6)) \\ \omega_2 U_c(\frac{2\pi}{3}, \frac{5\pi}{6}) + (1 - \omega_2) U_c(\frac{5\pi}{3}, \frac{11\pi}{6}), & \text{if } Z' = 2, X'_6 = I(X_6 \leq \text{median}(X_6)) \\ \omega_3 U_c(\frac{\pi}{3}, \frac{\pi}{2}) + (1 - \omega_3) U_c(\frac{4\pi}{3}, \frac{3\pi}{2}), & \text{if } Z' = 3, X'_9 = I(X_9 > \text{median}(X_9)) \\ \omega_3 U_c(\frac{5\pi}{6}, \pi) + (1 - \omega_3) U_c(\frac{11\pi}{6}, 2\pi), & \text{if } Z' = 3, X'_9 = I(X_9 \leq \text{median}(X_9)) \end{cases},$$

where $Z' = I(Z \leq z') + 2I(z' < Z \leq z'') + 3I(z'' > Z)$, and z', z'' are $\frac{1}{3}$ and

$\frac{2}{3}$ quantiles of Z , respectively.

The geodesic distance measures the dissimilarity of two directional observations.

The performances of the three screening procedures on Models (2.a) and (2.b) are exhibited in Table 2. From the results of (2.a) in Table 2, all methods are powerful in identifying the variables X_6, X_9 that have no interaction with the conditional variable; however, only the COME-CSIS is good at detecting the effective variable X_3 that has an interaction effect on Y . Furthermore, under Model (2.b), the CDC-SIS cannot select all influential variables simultaneously since distance covariance works on metric space satisfying a strong negative type condition (Lyons, 2013). Nevertheless, the COME-CSIS and BCor-SIS still have powerful performance, generally surpassing the BCor-SIS.

5. Screening of Corpus Callosum Shape. Imaging genetics has gradually become an up-and-coming field. Combining genetics and functional neuroimaging allows scientists to detect the association between neuroimaging phenotype and genetic variation. In this section, we analyze databases with imaging, genetic, and clinical data provided by the

TABLE 2
The selection proportion of effective variables in directional data

ρ	γ	Methods	Model (2.a)				Model (2.b)			
			P_3	P_6	P_9	P_a	P_3	P_6	P_9	P_a
0.0	d_1	CDC-SIS	0.64	0.99	0.99	0.62	0.04	0.00	0.00	0.00
	d_2	BCor-SIS	0.06	1.00	1.00	0.06	0.39	0.31	0.35	0.04
	d_3	COME-CSIS	0.96	0.92	0.96	0.85	0.76	0.70	0.69	0.36
	d_1	CDC-SIS	0.77	0.99	1.00	0.76	0.05	0.01	0.01	0.00
	d_2	BCor-SIS	0.08	1.00	1.00	0.08	0.59	0.48	0.54	0.18
	d_3	COME-CSIS	0.98	0.95	0.98	0.91	0.92	0.84	0.83	0.64
	d_1	CDC-SIS	0.83	1.00	1.00	0.83	0.07	0.01	0.01	0.00
	d_2	BCor-SIS	0.11	1.00	1.00	0.11	0.73	0.59	0.65	0.30
	d_3	COME-CSIS	0.99	0.97	0.99	0.95	0.94	0.90	0.92	0.78
0.7	d_1	CDC-SIS	0.61	1.00	1.00	0.61	0.01	0.01	0.01	0.00
	d_2	BCor-SIS	0.08	1.00	1.00	0.08	0.55	0.69	0.65	0.25
	d_3	COME-CSIS	0.93	1.00	0.99	0.93	0.54	0.79	0.81	0.37
	d_1	CDC-SIS	0.76	1.00	1.00	0.76	0.01	0.03	0.02	0.00
	d_2	BCor-SIS	0.15	1.00	1.00	0.15	0.75	0.87	0.83	0.55
	d_3	COME-CSIS	0.96	1.00	1.00	0.96	0.71	0.91	0.90	0.59
	d_1	CDC-SIS	0.80	1.00	1.00	0.80	0.02	0.05	0.03	0.00
	d_2	BCor-SIS	0.20	1.00	1.00	0.20	0.86	0.92	0.91	0.72
	d_3	COME-CSIS	0.96	1.00	1.00	0.96	0.79	0.96	0.92	0.71

Alzheimer’s Disease Neuroimaging Initiative (ADNI) study¹ to demonstrate the helpfulness of the COME-CSIS.

The corpus callosum is the largest white matter structure in the human brain, connecting the left and right hemispheres in the brain (Edwards et al., 2014). Anatomically, CC is roughly a 10 cm long, 1 cm wide curved structure in an adult human, containing approximately 200 million fibers. Standard anatomic divisions for CC are the rostrum, genu, body (including anterior and posterior parts), isthmus, and splenium (see Figure 2). Functionally, CC is essential for communication between the two cerebral hemispheres. It facilitates the integration of sensory and motor information from the two sides of the body and different influences on higher cognition related to social interaction and language. Since CC is an essential structural and functional part of the brain, finding the factors that impact its shape is valuable. Existing literature has shown that age and disease are related to CC shape (Hinkle, Fletcher and Joshi, 2014; Cornea et al., 2016; Fletcher, 2013; Joshi et al., 2013); However, the genetic factors influencing the CC shape have been largely undiscovered.

To this end, we analyze a preprocessed ADNI dataset (Cornea et al., 2016) containing CC shapes and demographics. The preprocessed dataset includes 371 subjects, where each subject’s gender, age, disease diagnosis (AD or health), CC’s shape and 6,995 single nucleotide polymorphisms (SNPs) are recorded. 50 two-dimensional points characterize the CC shape of each subject on the CC contour. Moreover, the dissimilarity between two shape observations are measured by Riemannian shape distance (Dryden and Mardia, 2016).

Next, we specify the explanatory variables and conditional variables in our analysis. Due to the difference in shape along the inner side of the posterior splenium and isthmus subregions for different age groups, it is concluded that age strongly influences the shape of CC contours (Cornea et al., 2016). Besides, Cornea et al. (2016) points out that the splenium seems less rounded, and the isthmus is thinner in subjects with AD than in HC. We conducted additional tests to assess the correlation between the CC shape and three variables: age, gender, and

¹adni.loni.usc.edu

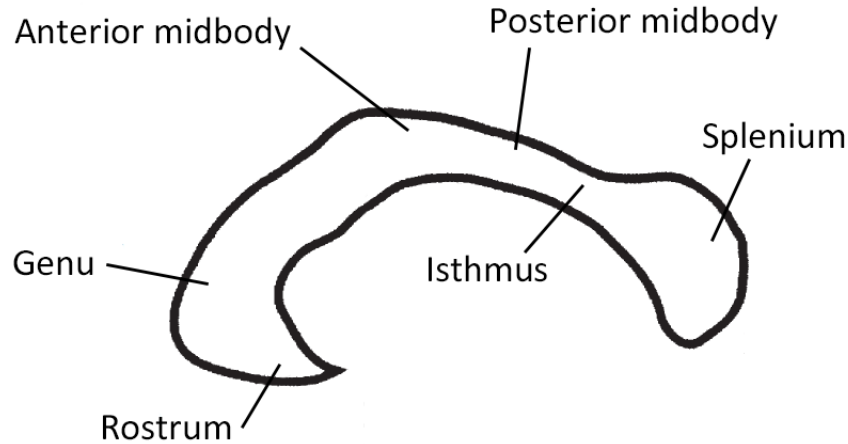


Fig 2: The image of midsagittal cut through the corpus callosum in [Eccher \(2014\)](#) with its major subunits from anterior to posterior: rostrum, genu, anterior midbody, posterior midbody, isthmus, and splenium.

disease status. These tests were performed using the ball covariance method with permutation replications 499 ([Pan et al., 2020](#)). The results are summarized in Table 3.

TABLE 3
P-values from correlation tests between CC shape and age, gender, and disease status

	Age	Gender	Disease status
p-value	0.01	0.09	0.02

At a significance level of 0.05, both age and disease status showed significant correlations with CC shape. In contrast, the correlation between gender and CC shape was not statistically significant. Given the two prior information, our interest is to detect the genetic factors associated with CC contour when controlling covariates age and group. Moreover, to verify the arguments that there is no significant gender effect on the CC shape after disease status and age are considered ([Cornea et al., 2016](#)), we treat gender as one of the explanatory variables in the screening procedure. We set $d_n = n/\log(n)$ and select the previously identified important SNPs for further analysis.

Table 4 lists the top 5 important SNPs selected for CC shape by the BCor-SIS, CDC-SIS, and COME-CSIS. From Table 4, the COME-CSIS and CDC-SIS select similar top-5 SNPs, but BCor-SIS selects quite different SNPs, This implies that considering the conditional variable greatly impacts the screening results. The SNP rs11668269, selected by the COME-CSIS and CDC-SIS, is in the LOC105372330 gene that is negatively correlated to APOE4+ males frontal white matter, where the APOE4 allele causes damage to the white matter of the corpus callosum ([Hsu et al., 2019](#); [Koizumi et al., 2018](#)).

The SNP rs4807022, initially identified through BCor-SIS, is within the gene encoding protein tyrosine phosphatase receptor sigma (PTPRS). This placement suggests a significant association with the CC shape. We conducted a hypothesis test on SNP rs4807022 with the conditional variables to further explore this relationship, employing ball covariance. The analysis yielded a p-value of 0.0267 for the association between the SNP and age, indicating a strong correlation. Conversely, the p-value for the association between the SNP and

Alzheimer’s Disease (AD) was 0.99, suggesting no significant dependence. We then segmented the data into age groups based on quantiles (55–72, 73–76, 77–80, and 81–95²) to examine variations across different age segments. This SNP data categorizes genetic variations as 0 (AA), 1 (Aa), and 2 (aa), representing two, one, and zero copies of the reference allele, respectively. The results, summarized in Table 5, reveal that the frequency of heterozygotes (1 for genotype Aa) increases with age. PTPRS has been implicated in the regulation of neurite outgrowth and has been shown to stimulate neurite outgrowth in response to the heparan sulfate proteoglycan GPC2, essential for normal brain development (Pulido et al., 1995; Coles et al., 2011). These functions suggest that PTPRS may play a role in longevity. Despite these findings, SNP rs4807022 is ranked 4808th in COME-CSIS, and when conditioned on age, the p-value derived from the COME analysis is 0.37. Overall, while there is a strong association between SNP rs4807022 and age, its link to CC shape appears to be mediated primarily through age-related changes rather than a direct genetic influence on CC shape.

Moreover, the COME-CSIS selects the SNP rs3745129 in the ZNF329 gene as the fourth important gene. Because an important paralog of the ZNF329 gene, ZFP37, expresses in all neurons of the central nervous system (Mazarakis et al., 1996), ZNF329 may influence the corpus callosum. Finally, the gender factor is ranked 4553 by the COME-CSIS, implying the gender effect is not significant after considering the age and disease status. This result is coincident with the finding of Cornea et al. (2016).

To further compare the performance of COME-CSIS and CDC-SIS, we randomly generated 1,000 noise SNP variables and identified the proportion of noise selected by the two methods. We begin by considering the Major Allele Frequency (p) and Minor Allele Frequency (MAF, q) in SNP noise, $p + q = 1$. We then generate the frequencies of the three genotypes (AA, Aa, aa) according to the Hardy-Weinberg Equilibrium (HWE). We conduct χ^2 test to check HWE, 5.86% of SNPs are rejected under significance level 0.05, which indicates that the SNPs in our dataset predominantly adhere to HWE, so it is reasonable to generate noise SNPs based on HWE. To simulate SNP noise, we employed two methods. The first method involved calculating the average MAF of 6,994 SNPs, found to be 45.9%, and subsequently generating 1,000 SNPs with MAF 45.9% to serve as noise. The second method consisted of randomly selecting 1,000 SNPs from the original set of 6,994 and generating noise based on their actual MAF. We conducted this experiment 20 times to ensure statistical reliability and counted the proportion of SNPs included in the noise under different settings of $d_n = \gamma \lceil n / \log(n) \rceil$, $\gamma = 1, 2, 3$. The results in Table 6 demonstrate that the COME-CSIS method selects a higher proportion of original, non-noise SNPs than CDC-SIS. This indicates that COME-CSIS is more robust and less affected by noise in the data. The superior performance of COME-CSIS is attributed to its utilization of rank-based distance metrics and local neighborhood structures, which significantly enhance its robustness against outliers and heavy-tailed distributions.

We visualize CC shapes in Figure 3 to gain more insight. Specifically, we divide the subjects into eight disjoint subsets according to their ages phase (55–72, 73–76, 77–80, and 81–95) and disease status (AD and HC), then, in each part of the subject, we demonstrate the Fréchet mean of CC shapes when the genetic factor takes different values. It can be observed that, for both of the top-2 SNPs selected by the COME-CSIS, they impact the CC shape condition on age and health status. More precisely, for the healthy subjects with age 72–76, the SNP rs11668269 with value AA associates with a smaller curvature in the body part of CC; for the AD patients with age 72–76, the SNP rs10410302 with value AA leads to a smaller curvature in the body part of CC.

²55, 72, 76, 80, and 92 are 0.0, 0.25, 0.5, 0.75, and 1.0 quantiles of the age, respectively.

TABLE 4
Top-5 selected variables for corpus callosum shape by different methods. SNP's corresponding genes are in parentheses if they exist

BCor-SIS	CDC-SIS	COME-CSIS
rs4807022 (PTPRS)	rs10414182	rs11668269 (LOC105372330)
rs8101539 (WDR88)	rs10424248	rs10414182
rs3786627 (ETFB)	rs11668269 (LOC105372330)	rs3786776 (PLA2G4C)
rs11085313	rs1979260 (MYO9B)	rs3745129 (ZNF329)
rs4805863	rs3786776 (PLA2G4C)	rs10518253

TABLE 5
SNP value in four age groups.

	55–72	73–76	77–80	81–95
AA	70	72	65	50
Aa	35	13	25	33
aa	1	2	2	2

TABLE 6
The average proportion of SNP noise selected by the two methods

Sampling mechanism	Method	63 ($\lceil n/\log(n) \rceil$)	126 ($2\lceil n/\log(n) \rceil$)	189 ($3\lceil n/\log(n) \rceil$)
Random	COME-CSIS	7.94%	9.60%	11.06%
	CDC-SIS	13.02%	13.57%	12.70%
Average	COME-CSIS	3.49%	7.14%	7.57%
	CDC-SIS	8.41%	8.89%	8.41%

In practical applications, COME-CSIS demonstrates enhanced capability in identifying key variables compared to methods that do not utilize conditional variables. By preemptively controlling for confounding factors such as age and gender, COME-CSIS allows for more accurate isolation and identification of core variables. Compared with other conditional variable screening methods (CDC-SIS), the COME-CSIS is more robust and less likely to select irrelevant noise. Consequently, this approach improves the robustness and reliability of the findings in complex analytical scenarios where multiple interdependent variables are present.

6. Conclusion and Discussion. We propose a conditional dependency measure named COME for metric spaces, which is capable of assessing both local and global dependencies. This model-free measure is adaptable to various complex non-Euclidean spaces. Although our initial analysis assumes X to be Euclidean, we can extend X to general metric space, provided that it satisfies the condition of being directionally limited. Additionally, we introduce a conditional screening method based on COME for ultra-high-dimensional space, proving its strong screening properties and offering theoretical support for practical applications.

Our method was employed to analyze genes associated with the shape of the corpus callosum. After integrating insights from both literature and data analysis, we utilized Alzheimer's Disease status and age as conditional variables Z , with CC shape as the response variable Y and gene as the predictor variable X . Most existing methods falter when applied to non-Euclidean response variables like CC shape. We identified the five most relevant SNPs for further analysis. The scientific validity of our SNP selection has been corroborated by existing research, which highlights connections to white matter and the APOE4+ allele. By contrasting our approach with non-conditional screening techniques like BCor-SIS, we demonstrated

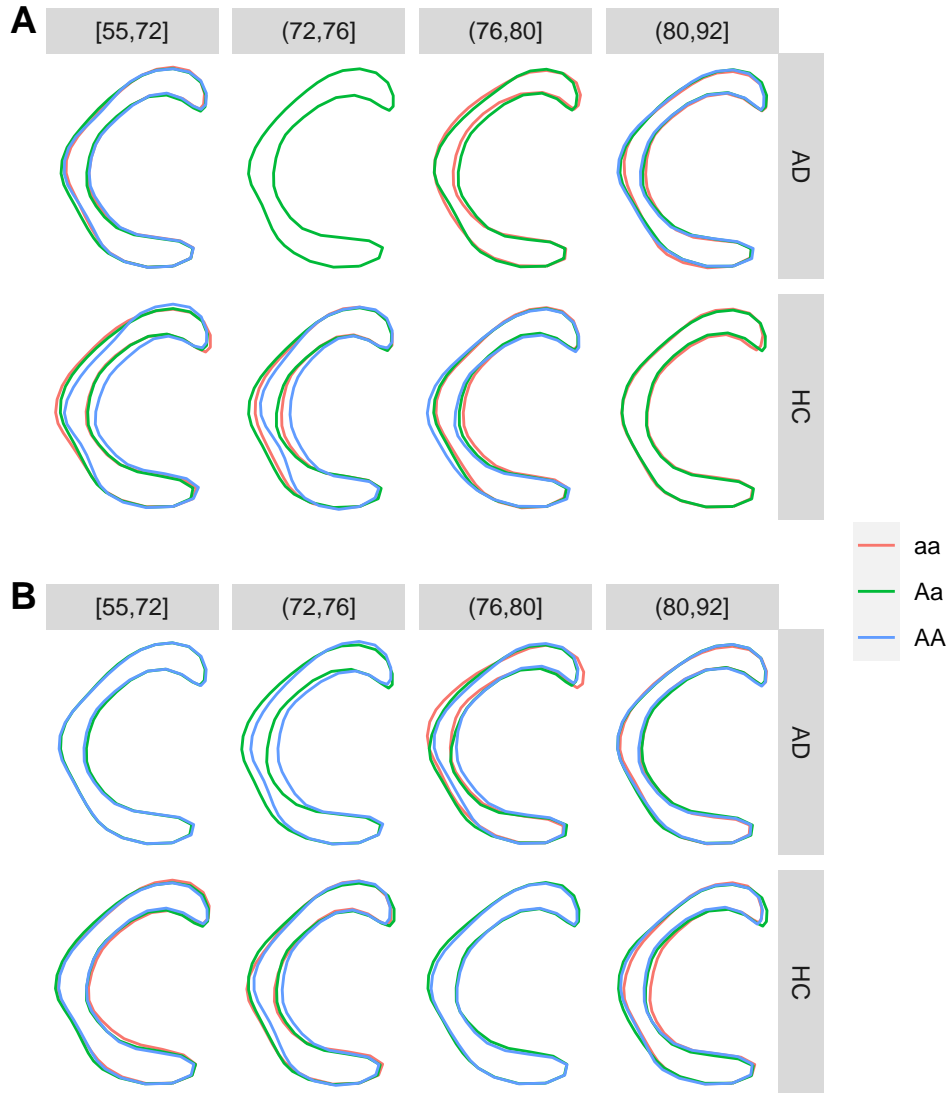


Fig 3: The corpus callosum (CC) shape in SNP rs11668269 (subfigure A) and rs10410302 (subfigure B). In each subfigure, the lower panels indicate healthy control, the upper panels indicate patients with Alzheimer's disease, and a column represents a specific age group. Four columns represent 55–72, 73–76, 77–80, and 81–95 years old, respectively. Ordinary Procrustes analysis (Dryden and Mardia, 2016) are conducted for all CC shapes.

that while the selected SNPs show strong correlations with factors such as age, they are not directly pivotal in influencing CC shape. Moreover, we simulated noisy SNPs based on the Hardy-Weinberg Equilibrium criterion, thereby demonstrating the robustness of COME-SIS and its capacity to mitigate the impact of irrelevant SNPs. Overall, in the context of CC shape-related gene analysis, COME-SIS proved effective and resilient in handling complex non-Euclidean response variables and high-dimensional predictor variables, showcasing broad potential for future applications.

Several issues warrant further investigation. The threshold used in our method is adopted from (Fan and Lv, 2008). It would be of interest to develop a criterion to determine the threshold for samples, which we leave as a subject for future research. Moreover, when processing

the response variable Z through kernel technology, we encounter the curse of dimensionality, particularly when Z is high-dimensional. This scenario is not uncommon, particularly when conditioning on a set of genes. Thus, developing advanced conditional analysis techniques to circumvent the curse of dimensionality represents a crucial direction for future research. Lastly, while we have successfully identified key SNPs in our real data analysis, it is also worthwhile to explore further analyses, such as predicting the shape of CC itself or developing more effective prognostic strategies.

Acknowledgments. The first two authors contributed equally and are listed in alphabetical order.

Dr. Wang’s research is partially supported by the National Natural Science Foundation of China (12231017, 72171216) and the National Key R&D Program of China (2022YFA1003803). Dr. Pan’s research is partially supported by the National Natural Science Foundation of China (12322113, 72495122, 12288201).

Data collection and sharing for this project was funded by the Alzheimer’s Disease Neuroimaging Initiative (ADNI) (National Institutes of Health Grant U01 AG024904) and DOD ADNI (Department of Defense award number W81XWH-12-2-0012). ADNI is funded by the National Institute on Aging, the National Institute of Biomedical Imaging and Bioengineering, and through generous contributions from the following: AbbVie, Alzheimer’s Association; Alzheimer’s Drug Discovery Foundation; Araclon Biotech; BioClinica, Inc.; Biogen; Bristol-Myers Squibb Company; CereSpir, Inc.; Cogstate; Eisai Inc.; Elan Pharmaceuticals, Inc.; Eli Lilly and Company; EuroImmun; F. Hoffmann-La Roche Ltd and its affiliated company Genentech, Inc.; Fujirebio; GE Healthcare; IXICO Ltd.; Janssen Alzheimer Immunotherapy Research & Development, LLC.; Johnson & Johnson Pharmaceutical Research & Development LLC.; Lumosity; Lundbeck; Merck & Co., Inc.; Meso Scale Diagnostics, LLC.; NeuroRx Research; Neurotrack Technologies; Novartis Pharmaceuticals Corporation; Pfizer Inc.; Piramal Imaging; Servier; Takeda Pharmaceutical Company; and Transition Therapeutics. The Canadian Institutes of Health Research is providing funds to support ADNI clinical sites in Canada. Private sector contributions are facilitated by the Foundation for the National Institutes of Health (www.fnih.org). The grantee organization is the Northern California Institute for Research and Education, and the study is coordinated by the Alzheimer’s Therapeutic Research Institute at the University of Southern California. ADNI data are disseminated by the Laboratory for Neuro Imaging at the University of Southern California.

SUPPLEMENTARY MATERIAL

Supplement A: Supplement for “Identification of Genetic Factors Associated with Corpus Callosum Morphology: Conditional Strong Independence Screening for Non-Euclidean Responses”

The Supplementary Material includes technical proof and the detail of the iterative COME-CSIS algorithm.

Supplement B: R code for “Identification of Genetic Factors Associated with Corpus Callosum Morphology: Conditional Strong Independence Screening for Non-Euclidean Responses”

R-package *come* containing code to perform the COME-CSIS described in the article and R scripts used to generate the numerical results presented in the paper.

REFERENCES

- BACHMAN, A. H., LEE, S. H., SIDTIS, J. J. and ARDEKANI, B. A. (2014). Corpus callosum shape and size changes in early Alzheimer’s disease: A longitudinal MRI study using the OASIS brain database. *Journal of Alzheimer’s Disease* **39** 71–78.

- BARUT, E., FAN, J. and VERHASSELT, A. (2016). Conditional Sure Independence Screening. *Journal of the American Statistical Association* **111** 1266-1277. PMID: 28360436. <https://doi.org/10.1080/01621459.2015.1092974>
- BISWAL, B. B., MENNES, M., ZUO, X.-N., GOHEL, S., KELLY, C., SMITH, S. M., BECKMANN, C. F., ADELSTEIN, J. S., BUCKNER, R. L., COLCOMBE, S., DOGONOWSKI, A.-M., ERNST, M., FAIR, D., HAMPSON, M., HOPTMAN, M. J., HYDE, J. S., KIVINIEMI, V. J., KÖTTER, R., LI, S.-J., LIN, C.-P., LOWE, M. J., MACKAY, C., MADDEN, D. J., MADSEN, K. H., MARGULIES, D. S., MAYBERG, H. S., MCMAHON, K., MONK, C. S., MOSTOFSKY, S. H., NAGEL, B. J., PEKAR, J. J., PELTIER, S. J., PETERSEN, S. E., RIEDL, V., ROMBOUTS, S. A. R. B., RYPMA, B., SCHLAGGAR, B. L., SCHMIDT, S., SEIDLER, R. D., SIEGLE, G. J., SORG, C., TENG, G.-J., VEIJOLA, J., VILLRINGER, A., WALTER, M., WANG, L., WENG, X.-C., WHITFIELD-GABRIELI, S., WILLIAMSON, P., WINDISCHBERGER, C., ZANG, Y.-F., ZHANG, H.-Y., CASTELLANOS, F. X. and MILHAM, M. P. (2010). Toward discovery science of human brain function. *Proceedings of the National Academy of Sciences* **107** 4734-4739. <https://doi.org/10.1073/pnas.0911855107>
- CHEN, X., ZHANG, Y., CHEN, X. and LIU, Y. (2019). A simple model-free survival conditional feature screening. *Statistics & Probability Letters* **146** 156-160.
- COLES, C. H., SHEN, Y., TENNEY, A. P., SIEBOLD, C., SUTTON, G. C., LU, W., GALLAGHER, J. T., JONES, E. Y., FLANAGAN, J. G. and ARICESCU, A. R. (2011). Proteoglycan-specific molecular switch for RPTP σ clustering and neuronal extension. *Science* **332** 484-488.
- CORNEA, E., ZHU, H., KIM, P. and IBRAHIM, J. (2016). Regression Models on Riemannian Symmetric Spaces. *Journal of the Royal Statistical Society: Series B (Statistical Methodology)* **79** n/a-n/a. <https://doi.org/10.1111/rssb.12169>
- DRYDEN, I. L. and MARDIA, K. V. (2016). *Statistical shape analysis: with applications in R* **995**. John Wiley & Sons.
- ECCHER, M. (2014). Corpus Callosum. In *Encyclopedia of the Neurological Sciences (Second Edition)* second edition ed. (M. J. Aminoff and R. B. Daroff, eds.) 867 - 868. Academic Press, Oxford. <https://doi.org/10.1016/B978-0-12-385157-4.01137-4>
- EDWARDS, T. J., SHERR, E. H., BARKOVICH, A. J. and RICHARDS, L. J. (2014). Clinical, genetic and imaging findings identify new causes for corpus callosum development syndromes. *Brain* **137** 1579-1613. <https://doi.org/10.1093/brain/awt358>
- FAN, J. and LV, J. (2008). Sure independence screening for ultrahigh dimensional feature space. *Journal of the Royal Statistical Society: Series B (Statistical Methodology)* **70** 849-911. <https://doi.org/10.1111/j.1467-9868.2008.00674.x>
- FEBRERO-BANDE, M. and DE LA FUENTE, M. (2012). Statistical Computing in Functional Data Analysis: The R Package fda.usc. *Journal of Statistical Software, Articles* **51** 1-28. <https://doi.org/10.18637/jss.v051.i04>
- FEDERER, H. (2014). *Geometric measure theory*. Springer.
- FLETCHER, P. T. (2013). Geodesic regression and the theory of least squares on Riemannian manifolds. *International journal of computer vision* **105** 171-185.
- FUKUMIZU, K., GRETTON, A., SUN, X. and SCHÖLKOPF, B. (2008). Kernel measures of conditional dependence. In *Advances in neural information processing systems* 489-496.
- HINKLE, J., FLETCHER, P. T. and JOSHI, S. (2014). Intrinsic polynomials for regression on Riemannian manifolds. *Journal of Mathematical Imaging and Vision* **50** 32-52.
- HONG, H. G., KANG, J. and LI, Y. (2018). Conditional screening for ultra-high dimensional covariates with survival outcomes. *Lifetime data analysis* **24** 45-71.
- HONG, H. G., WANG, L. and HE, X. (2016). A data-driven approach to conditional screening of high-dimensional variables. *Stat* **5** 200-212.
- HSU, M., DEDHIA, M., CRUSIO, W. and DELPRATO, A. (2019). Sex differences in gene expression patterns associated with the APOE4 allele. *F1000Research* **8**. <https://doi.org/10.12688/f1000research.18671.2>
- HU, Q. and LIN, L. (2017). Conditional sure independence screening by conditional marginal empirical likelihood. *Annals of the Institute of Statistical Mathematics* **69** 63-96.
- HU, W., HUANG, M., PAN, W., WANG, X., WEN, C., TIAN, Y., ZHANG, H. and ZHU, J. (2019). cdcsis: Conditional Distance Correlation Based Feature Screening and Conditional Independence Inference R package version 2.0.3.
- HUANG, D., LI, R. and WANG, H. (2014). Feature Screening for Ultrahigh Dimensional Categorical Data With Applications. *Journal of Business & Economic Statistics* **32** 237-244. <https://doi.org/10.1080/07350015.2013.863158>
- JOSHI, S. H., NARR, K. L., PHILIPS, O. R., NUECHTERLEIN, K. H., ASARNOW, R. F., TOGA, A. W. and WOODS, R. P. (2013). Statistical shape analysis of the corpus callosum in schizophrenia. *Neuroimage* **64** 547-559.

- KENNEDY, H., VAN ESSEN, D. C. and CHRISTEN, Y. (2016). *Micro-, meso- and macro-connectomics of the brain*. Springer Nature.
- KOIZUMI, K., HATTORI, Y., AHN, S. J., BUENDIA, I., CIACCIARELLI, A., UEKAWA, K., WANG, G., HILLER, A., ZHAO, L., VOSS, H. U. et al. (2018). Apo ϵ 4 disrupts neurovascular regulation and undermines white matter integrity and cognitive function. *Nature communications* **9** 1–11.
- LI, R., ZHONG, W. and ZHU, L. (2012). Feature Screening via Distance Correlation Learning. *Journal of the American Statistical Association* **107** 1129–1139. PMID: 25249709. <https://doi.org/10.1080/01621459.2012.695654>
- LIN, L. and SUN, J. (2016). Adaptive conditional feature screening. *Computational Statistics & Data Analysis* **94** 287–301. <https://doi.org/10.1016/j.csda.2015.09.002>
- LIU, Y. and CHEN, X. (2018). Quantile screening for ultra-high-dimensional heterogeneous data conditional on some variables. *Journal of Statistical Computation and Simulation* **88** 329–342.
- LIU, J., LI, R. and WU, R. (2014). Feature selection for varying coefficient models with ultrahigh-dimensional covariates. *Journal of the American Statistical Association* **109** 266–274.
- LU, S., CHEN, X. and WANG, H. (2019). Conditional distance correlation sure independence screening for ultra-high dimensional survival data. *Communications in Statistics-Theory and Methods* 1–18.
- LYONS, R. (2013). Distance Covariance in Metric Spaces. *The Annals of Probability* **41** 3284–3305. <https://doi.org/10.1214/12-AOP803>
- MAZARAKIS, N., MICHALOVICH, D., KARIS, A., GROSVELD, F. and GALJART, N. (1996). Zfp-37Is a Member of the KRAB Zinc Finger Gene Family and Is Expressed in Neurons of the Developing and Adult CNS. *Genomics* **33** 247–257. <https://doi.org/10.1006/geno.1996.0189>
- MEINSHAUSEN, N. and BUHLMANN, P. (2006). High-dimensional graphs and variable selection with the Lasso. *Ann. Statist.* **34** 1436–1462. <https://doi.org/10.1214/0090536060000000281>
- PAN, W., WANG, X., XIAO, W. and ZHU, H. (2019). A generic sure independence screening procedure. *Journal of the American Statistical Association* **114** 928–937.
- PAN, W., WANG, X., ZHANG, H., ZHU, H. and ZHU, J. (2020). Ball Covariance: A Generic Measure of Dependence in Banach Space. *Journal of the American Statistical Association* **115** 307–317. <https://doi.org/10.1080/01621459.2018.1543600>
- PETERSEN, A. and MÜLLER, H.-G. (2019). Fréchet regression for random objects with Euclidean predictors. *Ann. Statist.* **47** 691–719. <https://doi.org/10.1214/17-AOS1624>
- PULIDO, R., SERRA-PAGES, C., TANG, M. and STREULI, M. (1995). The LAR/PTP delta/PTP sigma subfamily of transmembrane protein-tyrosine-phosphatases: multiple human LAR, PTP delta, and PTP sigma isoforms are expressed in a tissue-specific manner and associate with the LAR-interacting protein LIP. 1. *Proceedings of the National Academy of Sciences* **92** 11686–11690.
- SHAH, R. D. and PETERS, J. (2020). The hardness of conditional independence testing and the generalised covariance measure. *Annals of Statistics* **48** 1514–1538. <https://doi.org/10.1214/19-AOS1857>
- TANAKA-ARAKAWA, M. M., MATSUI, M., TANAKA, C., UEMATSU, A., UDA, S., MIURA, K., SAKAI, T. and NOGUCHI, K. (2015). Developmental changes in the corpus callosum from infancy to early adulthood: a structural magnetic resonance imaging study. *PLoS one* **10** e0118760.
- VERMEULEN, C. L., DU TOIT, P. J., VENTER, G. and HUMAN-BARON, R. (2023). A morphological study of the shape of the corpus callosum in normal, schizophrenic and bipolar patients. *Journal of anatomy* **242** 153–163.
- WANG, X., PAN, W., HU, W., TIAN, Y. and ZHANG, H. (2015). Conditional Distance Correlation. *Journal of the American Statistical Association* **110** 1726–1734. PMID: 26877569. <https://doi.org/10.1080/01621459.2014.993081>
- WANG, X., ZHU, J., PAN, W., ZHU, J. and ZHANG, H. (2024). Nonparametric Statistical Inference via Metric Distribution Function in Metric Spaces. *Journal of the American Statistical Association* **119** 2772–2784. <https://doi.org/10.1080/01621459.2023.2277417>
- WEN, C., PAN, W., HUANG, M. and WANG, X. (2018). Sure independence screening adjusted for confounding covariates with ultrahigh dimensional data. *Statistica Sinica* 293–317.
- XUE, J. and LIANG, F. (2017). A Robust Model-Free Feature Screening Method for Ultrahigh-Dimensional Data. *Journal of Computational and Graphical Statistics* **26** 803–813. PMID: 30532512. <https://doi.org/10.1080/10618600.2017.1328364>
- ZHANG, S., PAN, J. and ZHOU, Y. (2018). Robust conditional nonparametric independence screening for ultrahigh-dimensional data. *Statistics & Probability Letters* **143** 95–101.
- ZHENG, Q., HONG, H. G. and LI, Y. (2020). Building generalized linear models with ultrahigh dimensional features: A sequentially conditional approach. *Biometrics* **76** 47–60.
- ZHU, J., PAN, W., ZHENG, W. and WANG, X. (2021). Ball: An R Package for Detecting Distribution Difference and Association in Metric Spaces. *Journal of Statistical Software, Articles* **97** 1–31. <https://doi.org/10.18637/jss.v097.i06>